

Comparison between 18650 Lithium-ion Cells of Different Composition Subjected to Thermal Abuse

Sofia Ubaldi, Paola Russo*

Dipartimento Ingegneria Chimica Materiali Ambiente, Sapienza Università di Roma, Via Eudossiana 18, Roma, Italy.
 paola.russo@uniroma1.it

Lithium-ion Batteries (LIBs) are characterized by high energy and power density and long life and are currently used in many applications from portable devices to energy storage systems. These features increase safety concerns, especially when these devices are subject to thermal, mechanical, or electrical abuse. Abuse can lead to exothermic reactions of cell components and with each other, causing a rapid increase in temperature, called Thermal Runaway (TR), and pressure. The response to abuse depends on the physical-chemical characteristics of Li-ion cells, such as chemical composition and State of Charge (SOC). To study the effect of chemical composition, three different 18650 Li-ion cells were tested, i.e., Lithium Titanate Oxide (*LTO*), Lithium Iron Phosphate (*LFP*) and Lithium Nickel Cobalt Aluminium Oxide (*NCA*), at the same SOC (100 %). The cells were subjected to thermal abuse tests in a tubular reactor connected at the output to an online Fourier-transform infrared spectroscopy (FT-IR). All events, i.e., Current Interrupt Device (CID) activation, venting and TR, were recorded, and the gases emitted were traced back to the reactions that take place inside the cell. By comparing the response of the cells with different composition it was found that onset of TR occurs at lower temperature for *NCA* than the other cells (207 vs 233-234 °C), but the maximum temperature reached during TR by the *NCA* is higher (579 vs 310-338 °C). Regarding toxic emissions, for all three cells the values of hydrofluoric acid (HF) and carbon monoxide (CO) significantly exceed the Immediately Dangerous to Life or Health Limit (IDLH) defined by the National Institute for Occupational Safety and Health set at 30 ppm for HF and 1200 ppm for CO in 30 min, with maximum concentration of HF between 824 - 893 ppm and the maximum concentration of CO changing according to the chemistries: 231990 ppm for *NCA*, 140728 ppm for *LTO* and 97140 ppm for *LFP*.

1. Introduction

Lithium-ion Batteries (LIBs) are secondary batteries and are currently applied in portable applications, such as smartphone, in mobility, such as electrical vehicles, and energy storage systems. LIBs are characterized by high energy density (100 - 200 Wh/kg), high power density (360 W/kg) and long life (500 - 2000 cycles) (Williamson et al., 2011), but according to the application the technical specification required changed and the chemical composition too. The most common cell cathode chemistries available on the market are Lithium Iron Phosphate (LiFePO_4 , *LFP*), Lithium Nickel Cobalt Aluminium Oxide (LiNiCoAlO_2 , *NCA*), Lithium Cobalt Oxide (LiCoO_2 , *LCO*), Lithium Nickel Manganese Cobalt Oxide (LiNiMnCoO_2 , *NMC*) and Lithium Manganese Oxide (LiMn_2O_4 , *LMO*), while the chemical composition of the anode can be Lithium Titanate Oxide (Li_2TiO_3 , *LTO*) or graphite (Kaliaperumal et al., 2021). Table 1 reported the technical specifications for commercial cells (Battery University, 2021).

Table 1: Technical specifications for commercial cells (Battery University, 2021)

Specification	<i>LTO</i>	<i>LFP</i>	<i>LCO</i>	<i>NCA</i>	<i>NMC</i>	<i>LMO</i>
Nominal voltage (V)	2.40	3.20 - 3.30	3.60	3.6	3.6 - 3.7	3.7
Typical voltage (V/cell)	1.80 - 2.85	2.50 - 3.65	3.00 - 4.20	3.0 - 4.2	3.0 - 4.2	3.0 - 4.2
Specific energy or capacity (Wh/kg)	50 - 80	90 - 120	150 - 200	200 - 260	150 - 220	100-150

High energy and power densities increase the safety concerns, especially when these devices are subjected to an electrical, mechanical or thermal abuse (Kaliaperumal et al., 2021). The electrical abuse can be induced both from external, such as over or under voltage values, or internal, such as Li-metal dendrite, short circuiting. The mechanical abuse is usually induced by the deformation of the external case of the cell, such as penetration, while the thermal abuse can be caused by an external heating source near the cell. All these abuses lead to a change in chemical composition, by exothermic reactions between internal components (Xu et al., 2021), an increase in internal temperature and pressure, with consequent activation of safety devices, such as the Current Interrupt Device (CID) activation and the vent valve opening (Li et al., 2020). Since these are exothermic reactions, in the case of not efficient heat exchange with the environment, the temperature of the system can increase drastically in a short time causing the Thermal Runaway (TR) with release of gases, solids, fire and/or explosion (Lopez et al., 2015). The temperature, pressure, and product composition mainly depend on the physical-chemical characteristics of the Li-ion cells, such as chemical composition (Barkholtz et al., 2019) and State of Charge (SOC) (Kvasha et al., 2018).

Tolerance to thermal abuse can be studied using calorimetric techniques on both whole cells and single cell components (Roth, 2004). Differential scanning calorimetry (DSC) on the single components allows to have the onset temperature and the enthalpy of the reactions that take place during heating (Mele et al., 2022). The combination of calorimetric analysis for cell components and single cell allows to correlate the contributions of the cell components to the TR response of the cell (Kvasha et al., 2018). By comparing the different chemical compositions of the cathode, it was found that *LFP* is the most thermally stable while *NCA*, *NCM* and *LCO* are the most reactive and have poorer thermal stability (Kvasha et al., 2018). The higher stability of *LFP* is due to strong P-O covalent bonds in $(\text{PO}_4)^{3-}$ polyanion compared to *NCA* and *NCM* which decompose at lower temperatures with release of oxygen from the crystal lattice structure, which induced a chain of exothermic reactions. For the anode, *LTO* is more stable than graphite due to the inherent thermal stability of the $\text{Li}_4\text{Ti}_5\text{O}_{12}$ material compared to graphite layers (Kvasha et al., 2018). Therefore, it emerged that the most stable materials are those in *LFP* and *LTO*, while *LCO*, *NCA* and *NMC* materials show lower thermal stability. Regarding the whole cell, the onset temperature of the whole cell by accelerating rate calorimeter was typically observed at lower temperatures than onset temperatures of the cathodes decomposition reactions, obtained by DSC (Barkholtz et al., 2019). This is due to the lower thermal stability of the other components of the cells, such as the anode, in the case of graphite, of the electrolyte solution (Eshetu et al., 2013) and the plastic separator (Kvasha et al., 2018). In fact, the electrolyte solution is usually composed of flammable components, such as ethylene carbonate (EC), dimethyl carbonate (DMC), diethyl carbonate (DEC), ethyl acetate (EA) and relative mixtures. The range values of boiling temperature for those compounds are between 77 °C (EA) and 248 °C (EC) while the flash points are significantly lower, in the range from -3 °C (EA) to 143 °C (EC) (Eshetu et al., 2013). Hence, the liquid electrolyte contributes to the total energy that can be generated due to TR driven combustion process (Eshetu et al., 2013). The role of the separator must also be evaluated, in fact during heating the plastic separator melts causing an internal short circuit that accelerates the TR of the cell (Kvasha et al., 2018). Another parameter that affects the response to thermal abuse of the cell is the SOC. In the case of single-component material there is a different behavior according to the chemical composition. The graphite anode and the *NCA* cathode show a drastic intensification of exothermic reactions with increasing SOC (Barkholtz et al., 2019). While *LTO* and *LFP* exhibit a similar trend regardless of SOC (Kvasha et al., 2018). It emerged that the *LFP* and *LTO* are very safe batteries even when fully charged, while for *LCO*, *NCA* and *NMC* a higher SOC favours the TR (Battery University, 2021). Therefore, higher SOC results in higher temperature during TR with lower onset temperature (Barkholtz et al., 2019). A safety aspect that also must be considered is that flammable and toxic gases may be produced during TR (Sun et al., 2016). The main gases emitted during a thermal abuse test are carbon monoxide (CO), carbon dioxide (CO₂), methane (CH₄), fluorinated compounds, such as hydrofluoric acid (HF), and the electrolytic solvents (Golubkov et al., 2015). Most of these gases are dangerous to humans and environment. Both the chemical composition and the SOC may influence the products emitted and the relative quantities. Regardless of the anode and cathode composition, in the case of the LIBs with liquid electrolyte the greatest hazard is the generation of fluoride gas emissions, such as HF, phosphoryl fluoride (POF₃) and phosphorus pentafluoride (PF₅), which are due to the decomposition of Li-salt, such as hexafluorophosphate (LiPF₆) (Larsson et al., 2017). The total quantities emitted increase with higher SOC, indeed 100 % is the most hazardous SOC in terms also of toxicity (Sun et al., 2016).

To investigate the effect of chemistry on behaviour under thermal abuse, three different cylindrical Li-ion cells (*LTO*, *LFP* and *NCA*) at the same SOC, 100 %, were investigated. The cells were subjected to thermal abuse in a tubular reactor connected to an online Fourier-transform infrared spectroscopy (FT-IR). Cell temperature, pressure and related emitted gases were monitored by thermocouples, pressure gauge and FT-IR, to correlate the thermal abuse response of the cells, such as CID-activation, venting and TR, to the reaction products emitted. So, the different cells are compared to define the safest of those Li-ion cells in terms of temperature of

TR and gases compositions, compared with the Immediately Dangerous to Life or Health Limit (IDLH), to have a more comprehensive understanding on the dangerousness of cells when subjected to thermal abuse.

2. Material and Methods

2.1 Material

Figure 1 illustrated the cylindrical lithium-ion cells, 18650, considered in this study (a) Lithium Nickel Cobalt Aluminium Oxide (*NCA*), (b) Lithium Titanate Oxide (*LTO*) and (c) Lithium Iron Phosphate (*LFP*) with their chemical composition and technical specifications.




(a)		Parameter	
		Chemistry	Graphite (anode); NCA (cathode)
		Rated capacity (mAh)	Min. 3200
		Nominal voltage (V)	3.6
		Weight (g)	48.5
(b)		Parameter	
		Chemistry	LTO (anode); LMO (cathode)
		Rated capacity (mAh)	Min. 1300
		Nominal voltage (V)	2.4
		Weight (g)	40.0
(c)		Parameter	
		Anode chemistry	Graphite (anode); LFP (cathode)
		Rated capacity (mAh)	Min. 1300
		Nominal voltage (V)	3.2
		Weight (g)	40.0

Figure 1: Chemical composition and technical specifications of Li-ion cells: (a) *NCA*; (b) *LTO*; (c) *LFP*

Before tests, a standard procedure consisting of five charge-discharge cycles for the formation of the Solid Electrolyte Interface (SEI) was carried out on the cells using a PS 8000 2U series power supply from Elektro-Automatik. Then the cells were charged using a PS 8000 2U series power supply from Elektro-Automatik. The cells were charged to the maximum SOC (100 %), setting the maximum voltage according to the specifications, so 4.20 V for *NCA*, 2.80 V for *LTO* and 3.70 V for *LFP* (Figure 1).

2.2 Methods: Thermal abuse test

Thermal abuse tests were conducted in a laboratory reactor with an inlet airflow of 500 Nml/min over a temperature range of 20 to 400 °C, with a heating rate of 5 °C/min. When the TR condition is reached, the oven is switched off. Two thermocouples, TC₁ and TC₂, were positioned on the cell surface for monitoring cell temperature and a pressure transducer in the reactor for monitoring pressure changes. An online Fourier-transform infrared spectroscopy (FT-IR, Spectrum 3, Perkin Elmer) was connected to the reactor outlet to continuously monitor the emitted gases. The spectra were collected at the following spectrometric parameters, a resolution of 4 cm⁻¹ in the spectral range between 4500 cm⁻¹ and 650 cm⁻¹ with a scan/spectrum of 8 and detected by the mercury cadmium telluride (MCT) detector. Identification and quantification were obtained using standard spectra and calibration lines, obtained using SpectrumQuant software (Perkin Elmer). The characteristics of the reactor, acquisition and quantification procedure are better specified in the study of Ubaldi et al. (2023). Test were carried out on cells at 100 % SOC.

3. Results

For each thermal abuse test, the temperature and pressure of the three key events were defined: i) CID-activation, ii) venting and iii) TR. The first event is the activation of the CID due to the increase in internal pressure of the cell (at about 10 bar), which leads to the opening of the circuit with electrical insulation of one of the electrodes (Xu et al., 2021). Then the venting occurs (at about 20 bar), with the emission of vapor/gas from the vent valve due to the increase in pressure inside the cell (Li et al., 2020). TR refers to the moment in which the temperature increases with a self-heating rate greater than 10 °C/min. Figure 3 illustrated the temperature and pressure profile during the test of *LTO* cell. It is possible to identify at 2484 s the venting, with a correspondent increase in pressure due to gas/vapor release form the cell into the rector and a slight decrease of the cell temperature due to the vaporization of the electrolyte released. While at about 2800 s the TR onset

is observed with a rapid increase in temperature and pressure. Table 2 summarized the average cell surface temperature ($^{\circ}\text{C}$) and pressure (barg) of the key events for the three cells.

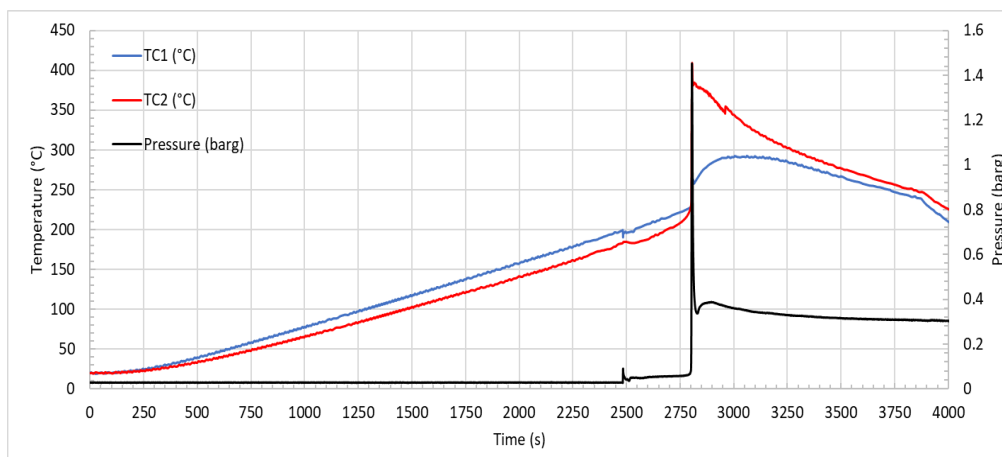


Figure 2: Temperature and pressure profile for test at 5 $^{\circ}\text{C}/\text{min}$ on LTO cell

Table 2: Temperature surface ($^{\circ}\text{C}$) and pressure (barg) of the key events (CID-activation, venting and TR) for the thermal abuse test on NCA, LTO and LFP

	CID-activation		Venting		TR onset		Peak	
	T ($^{\circ}\text{C}$)	P (barg)	T ($^{\circ}\text{C}$)	P (barg)	T ($^{\circ}\text{C}$)	P (barg)	T ($^{\circ}\text{C}$)	P (barg)
NCA	130 \pm 5	0.028	157 \pm 2	0.030	207 \pm 3	0.034	579 \pm 137	5.071
LTO	n.d.	n.d.	187 \pm 4	0.089	233 \pm 8	0.060	338 \pm 100	1.446
LFP	164 \pm 3	0.045	197 \pm 1	0.073	234 \pm 12	0.080	310 \pm 41	0.108

n.d.: not detected.

Comparing the results reported for the different cells (Table 2), the CID-activation occurs at lower temperatures for NCA cell than for LFP cell and it is not detected for LTO cell. For venting temperature, the value for NCA is lower than those measured for LTO, which is in turn lower than that for LFP. While for TR onset LFP and LTO have similar values but always higher than the NCA cell. These results agree with the higher stability of LFP and LTO cells with respect to NCA cell. Moreover, the development of the runaway reactions for the NCA cell generate a peak temperature (and pressure) significantly higher (more than 200 $^{\circ}\text{C}$) than the other cells.

In addition to the increase in temperature and pressure, thermal abuse also causes the emission of gases. Figure 3 illustrated the profiles of (a) HF and (b) CO, the most toxic reaction products, produced by the three cells. The hydrofluoric acid (HF) is produced by the degradation reaction of the lithium salt LiFP_6 used in the electrolyte solution while CO by the decomposition of the solvents (EC and DMC) in the electrolyte solution which is then oxidized to CO_2 . At the CID-activation for the NCA cell, there is an increase in the concentration of HF. Then both HF and CO concentrations increase for all the tested cells when venting occurs (at 2770 s for NCA, 2484 s for LTO and 2488 s for LFP), reach a maximum at the TR (at 3122 s for NCA, 2803 s for LTO and for 2658 s LFP) and decrease as the temperature decreases. The peak value of HF (about $8.5 \cdot 10^2$ ppm) is three orders of magnitude lower than the value measured for CO (about $1.9 \cdot 10^5$ ppm).

By integrating the area under the curve it is possible to obtain the average concentration of the gases emitted by each cell. 30 min was considered as integration period to be able to compare the values obtained with the Immediately Dangerous to Life or Health (IDLH) limits reported by the National Institute for Occupational Safety and Health (NIOSH). The total quantities, expressed in ppm, of HF and CO for the various cells are reported in Table 3. So, the average concentration values significantly exceed the IDLH values reported by the NIOSH set at 30 ppm for HF and 1200 ppm for CO in 30 min (NIOSH, 2023).

Table 3: Average concentration of HF and CO (ppm) emitted in 30 min during tests on NCA, LTO and LFP cell

Cell	HF (ppm)	CO (ppm)
NCA	100	15221
LTO	184	18009
LFP	200	10952

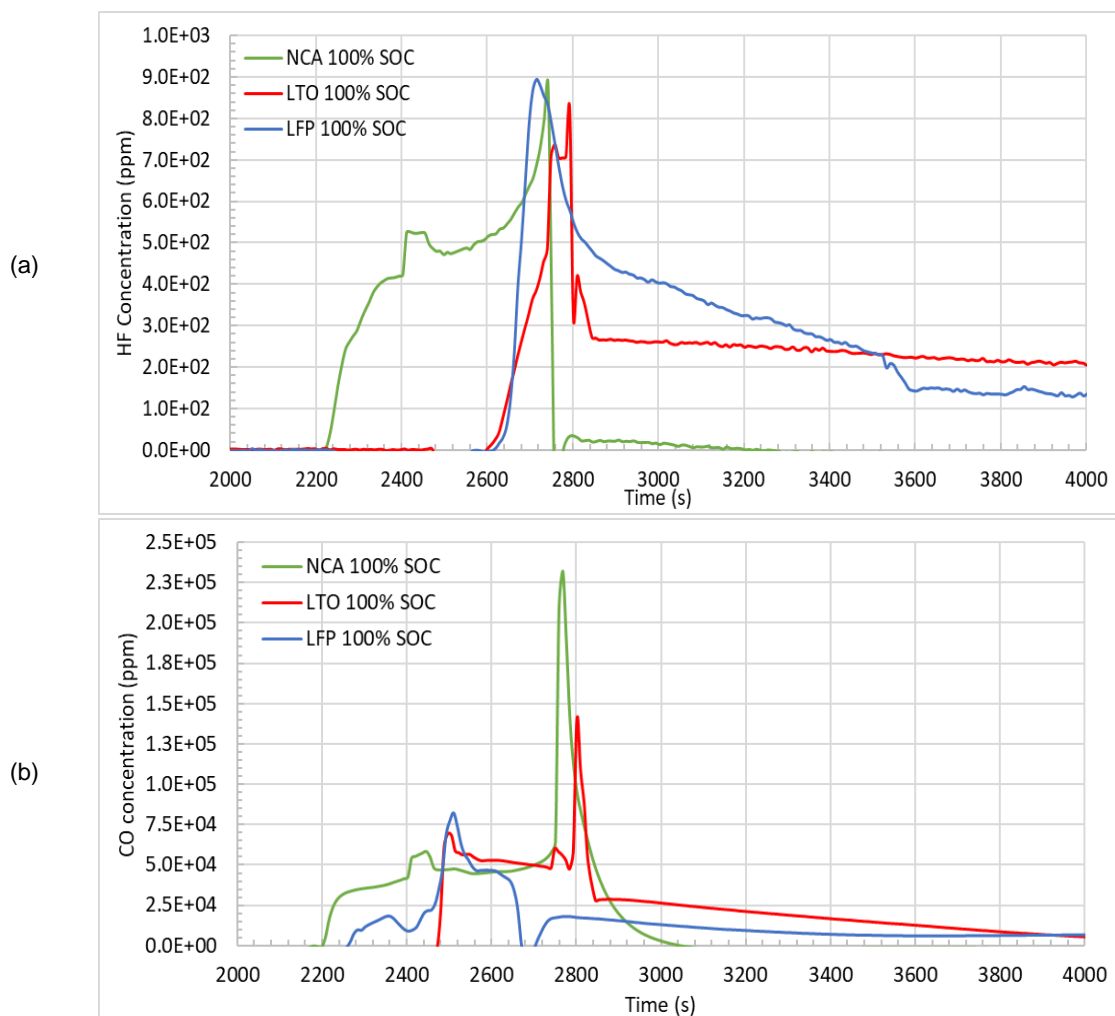


Figure 3: Concentration of (a) HF and (b) CO during thermal abuse tests for the three cells: (green line) NCA; (red line) LTO; (blue line) LFP

4. Conclusions

Thermal abuse tests were conducted on *NCA*, *LTO* and *LFO* cylindrical cells at 100 % SOC. In terms of temperature, the values recorded for the key events, CID-activation, venting and TR, are different according to the chemical composition, in fact, the venting and the TR occur at lower temperatures for *NCA* (157 °C and 207°C) than *LTO* (187 °C and 233 °C) and *LFP* (197 °C and 234 °C), respectively. The major differences were observed between the maximum temperature values reached during the thermal runaway: significantly higher for *NCA* (579 °C) than for *LTO* and *LFP* (338 °C and 310 °C, respectively).

The hazard of LIBs is not just correlated to the temperature, but also to the gas emitted both in terms of composition and quantity. The CO and HF concentration values were compared with the Immediately Dangerous to Life or Health (IDLH) defined by the National Institute for Occupational Safety and Health (NIOSH) to evaluate the dangerous for human health. The maximum values obtained for CO and HF for the three chemistries analyzed are significantly higher than these limits in the maximum point, TR, but the average concentration values obtained in 30 min are lower than the set values of 30 ppm for HF and 1200 ppm for CO. In conclusion, comparing the different cells it can be recognized that the most thermally stable lithium-ion cell is the *LTO* for the highest temperature necessary to activate the first key event, venting around 187 °C. While, in terms of toxicity there is no safer cell because the concentration values for both CO and HF significantly exceed the safety limits imposed by NIOSH.

The combination of all these results is fundamental for the complete understanding and related risk management of LIBs when they are involved in fires. These results can be used to identify the personal protective equipment that can be adopted by firefighters who must operate on the scene of a LIBs fire to be able to operate in complete safety.

Acknowledgments

This study was carried out within the MOST – Sustainable Mobility Center and received funding from the European Union Next-GenerationEU (PIANO NAZIONALE DI RIPRESA E RESILIENZA (PNRR) – MISSIONE 4 COMPONENTE 2, INVESTIMENTO 1.4 – D.D. 1033 17/06/2022, CN00000023). This manuscript reflects only the authors' views and opinions, neither the European Union nor the European Commission can be considered responsible for them.

References

- Barkholtz H.M., Preger Y., Ivanov S., Langendorf J., Torres-Castro L., Lamb J., Chalamala B., Ferreira S.R., 2019, Multi-scale thermal stability study of commercial lithium-ion batteries as a function of cathode chemistry and state-of-charge, *Journal of Power Sources*, 435, 226777. <https://doi.org/10.1016/j.jpowsour.2019.226777>.
- BU-205: Types of Lithium-ion, 2021, Battery University <<https://batteryuniversity.com/article/bu-205-types-of-lithium-ion>> accessed 28.02.2023.
- Eshetu G.G., Grugeon S., Laruelle S., Boyanov S., Lecocq A., Bertrand J.-P., Marlair G., 2013, In-depth safety-focused analysis of solvents used in electrolytes for large scale lithium ion batteries, *Phys. Chem. Chem. Phys.*, 15, 9145-9155. <https://doi.org/10.1039/c3cp51315g>.
- Golubkov A.W., Scheikl S., Planteu R., Voitic G., Wiltsche H., Stangl C., Fauler G., Thaler A., Hacker V., 2015, Thermal runaway of commercial 18650 Li-ion batteries with LFP and NCA cathodes – impact of state of charge and overcharge, *Royal Society of Chemistry Advances*, 5, 57171-57186. <https://doi.org/10.1039/c5ra05897j>.
- Kaliaperumal M., Dharanendrakumar M.S., Prasanna S., Abhishek K.V., Chidambaram R.K., Adams S., Zaghib K., Reddy M.V., 2021, Cause and Mitigation of Lithium-Ion Battery Failure—A Review, *Materials*, 14, 5676. <https://doi.org/10.3390/ma14195676>.
- Kvasha A., Gutiérrez C., Osa U., de Meaza I., Blazquez J.A., Macicior H., Urdampilleta I., 2018, A comparative study of thermal runaway of commercial lithium ion cells, *Energy*, 159, 547-557. <https://doi.org/10.1016/j.energy.2018.06.173>.
- Larsson F., Andersson P., Blomqvist P., Mellander B.-E., 2017, Toxic fluoride gas emissions from lithium-ion battery fires, *Scientific Reports*, 7:10018. <https://doi.org/10.1038/s41598-017-09784-z>.
- Li W., Crompton K.R., Hacker C., Ostanek J.K., 2020, Comparison of Current Interrupt Device and vent Design for 18650 Format Lithium-ion Battery Caps, *Journal of Energy Storage*, 32, 101890. <https://doi.org/10.1016/j.est.2020.101890>.
- Lopez C.F., Jeevarajan J.A., Mukherjee P., 2021, Characterization of Lithium-Ion Battery Thermal Abuse Behavior Using Experimental and Computational Analysis, *Journal of The Electrochemical Society*, 162 (10) A2163-A2173. <https://doi.org/10.1149/2.0751510jes>.
- Mele M.L., Bracciale M.P., Ubaldi S., Santarelli M.L., Mazzaro M., Di Bari C., Russo P., 2022, Thermal Abuse Tests on 18650 Li-Ion Cells Using a Cone Calorimeter and Cell Residues Analysis, *Energies*, 15, 2628. <https://doi.org/10.3390/en15072628>.
- Immediately Dangerous To Life or Health (IDLH) Values, The National Institute for Occupational Safety and Health (NIOSH) <<https://www.cdc.gov/niosh/idlh/intridl4.html>> accessed 20.03.2023.
- Roth E.P., Doughty D.H., 2004, Thermal abuse performance of high-power 18650 Li-ion cells, *Journal of Power Sources*, 128, 308-318. <https://doi.org/10.1016/j.jpowsour.2003.09.068>.
- Sun J., Li J., Zhou T., Yang K., Wei S., Tang N., Dang N., Li H., Qiu X., Chen L., 2016, Toxicity, a serious concern of thermal runaway from commercial Li-ion battery, *Nano Energy*, 27, 313-319. <http://dx.doi.org/10.1016/j.nanoen.2016.06.031>.
- Ubaldi S., Conti M., Marra F., Russo P., 2023, Identification of Key Events and Emissions during Thermal Abuse Testing on NCA 18650 Cells, *Energies*, 16, 3250. <https://doi.org/10.3390/en16073250>.
- Williamson S.S., Cassani P.A., Lukic S., Blunier B., 2011, *Power Electronics Handbook - devices, circuits, and applications* (Third Edition), Butterworth-Heinemann, 1331-1356. <https://doi.org/10.1016/B978-0-12-382036-5.00046-X>.
- Xu B., Kong L., Wen G., Pecht M.G., 2021, Protection Devices in Commercial 18650 Lithium-Ion Batteries, *IEEE*, 9, 66687-66695. <https://doi.org/10.1109/ACCESS.2021.3075972>.